COMENIUS UNIVERSITY OF BRATISLAVA
FACULTY OF MATHEMATICS AND PHYSICS

UNIBA-P1/94
February 1994

ARES - a spectrometer for investigation of rare particle decays and rare nuclear processes

V. A. Baranov[a], N. N. Chernyavski[a], P. G. Evtukhovich[b], A. I. Filippov[a], A. P. Fursov[a], A. A. Glazov[a], N. V. Khomutov[a], I. V. Kisel[a], A. S. Korenchenko[a], S. M. Korenchenko[a], B. F. Kostin[a], N. P. Kravchuk[a], N. A. Kuchinsky[a], A. S. Moiseenko[a], D. A. Mzhavia[c], K. G. Nekrasova[a], P. Povinec[d*], J. Szarka[d], V. S. Smirnov[a], Z. B. Tsamalaidze[c], J. Vanko[d], S. I. Yakovlev[a] and F. E. Zyazyulya[b]

[a] *Laboratory of Nuclear Problems, JINR, Dubna, Russia*
[b] *Institute of Physics, BAS, Minsk, Belorus*
[c] *Institute of High Energy Physics, Tbilisi University, Tbilisi, Georgia*
[d] *Department of Nuclear Physics, Comenius University, 84215 Bratislava, Slovakia*

A magnetic spectrometer intended for wide range of investigations of rare particle and nuclear processes is described. The spectrometer consists of cylindrical proportional chambers (~15000 signal wires) with gas supply and gas leakage systems, cylindrical scintillation hodoscopes, a magnet, electronics with power supplies, and data acquisition system. Basic characteristics of the spectrometer are discussed and results of first physics experiments are presented.

* Now at The International Atomic Energy Agency, MEL, 98012 Monaco

1. Introduction

There has been increasing interest in recent years in studying rare decays of muons and pions and rare nuclear processes [1]. Processes forbidden in the standard model of electroweak interactions by the law of muon number conservation, such as $\mu \rightarrow 3e$, $\mu \rightarrow e\gamma$, $\mu^- A \rightarrow e^- A^*$, have been of special interest [2-4]. To search for such rare processes that could originate with a probability of the order of $< 10^{-10}$ requires to use very sensitive detection systems and intense pion and muon beams. The detectors should work in high intensity beams with high registration efficiency, multiparticle registration capability and particle charge and energy determination. The detection systems should have high time and space resolution with a maximum solid angle [5].

For investigation of rare particle decays and rare nuclear processes a spectrometric facility ARES (Analyser of Rare Events) was designed and built in the Laboratory of Nuclear Problems of JINR (Dubna) on the meson beam of the JINR phasotron. The spectrometer is of universal construction and it has been designed for investigation of these processes:

(i) a study of rare muon decays and processes forbidden by the law of muon number conservation, such as $\mu^+ \rightarrow e^+ e^- e^+$, $\mu^+ \rightarrow e^+ \gamma$, $\mu^+ \rightarrow e^+ 2\gamma$, $\mu^- A \rightarrow e^+ A^*$;

(ii) a study of muon decays, such as $\mu^+ \rightarrow e^+ \nu_e \overline{\nu_\mu}$, $\mu^+ \rightarrow e^+ \nu_e \overline{\nu_\mu} \gamma$, $\mu^+ \rightarrow e^+ \nu_e \overline{\nu_\mu} e^+ e^-$;

(iii) a study of electroweak decays of pions, such as $\pi^+ \rightarrow e^+ \nu_e \gamma$, $\pi^+ \rightarrow e^+ \nu_e e^+ e^-$;

(iv) a study of π^0 decays, such as $\pi^0 \rightarrow e^+ e^-$, $\pi^0 \rightarrow e^+ e^- e^+ e^-$, $\pi^0 \rightarrow e^+ e^- \gamma$;

(v) a study of the process $\mu^- p \rightarrow n \nu_\mu \gamma$;

(vi) a study of rare reactions of pions and muons with nuclei.

The main detection problems associated with investigation of these processes are very low decay probabilities, high background and multiparticle environment.

2. The ARES spectrometer

The ARES spectrometer is a system of coaxial cylindrical proportional chambers and cylindrical scintillation hodoscopes placed in a magnetic field. The spectrometer consists of these main parts:

(i) detection part formed by cylindrical proportional chambers (15000 signal wires), 3 cylindrical scintillation hodoscopes (36 counters), a converter and a target,

(ii) proportional chamber electronics, electronics for photomultipliers, and a fast trigger electronics,

(iii) system of CAMAC modules for data readout, amplitude and time analysis,

(iv) data filtering system,

(v) computers,

(vi) magnet (SP-173), producing a homogeneous magnetic field for the detector (up to 1.8 T),

(vii) auxiliary equipment: a gas supply system with a gas leakage alarm, communications, power supplies, control systems, etc.

The main characteristics of the ARES spectrometer are given in table 1. The cross section of the spectrometer is shown in fig. 1. The central zone of the

spectrometer is left for target and for passing the beam. Various targets can be used according to the tasks of an experiment. It is possible to install, if necessary, a cylindrical gamma-converter, providing a detection of γ-quanta by electron-positron conversion pairs. The spectrometer enables to work with fluxes up to $\sim 10^7$ s^{-1} of stopping particles in a target and can be used in a complex trigger system.

The scheme of the detection part of the spectrometer is shown in fig. 2. The spectrometer consists of two main detection parts - the cylindrical proportional chambers and the cylindrical scintillation hodoscopes. The detection part of the spectrometer is 1060 mm in diameter and 600 mm long.

2.1. The cylindrical proportional chambers

The proportional chambers should enable an accurate registration of particle tracks, as the momentum of charged particles is determined from the track radius (the azimuthal and axial accuracy should be at least ± 1 and $\pm$ 2 mm, respectively), with high registration efficiency ($\sim$99 %), and they should have perfect long-term performance, as experiments are running for a long time and a change of a broken chamber would cause serious problems. As the main particles to be registered in chambers are electrons and positrons a low amount of matter on the track is required.

The main coordinate detectors of the ARES facility are composed of 18 cylindrical proportional chambers (CPC) with minimum matter on the particle tracks [6]. The main advantages of the CPC are a large solid angle and isotropy of properties in the plane perpendicular to the chamber axis. They allow the target to be completely surrounded by the working volume of the chambers and provide highly efficient systems for triggering, readout and background reduction.

There are two types of chambers - the chambers providing the azimuthal coordinate only (the accuracy ± 1 mm), and the chambers providing both the azimuthal and axial coordinates (the accuracy for the axial coordinate is ± 2 mm).

2.1.1. The construction of chambers

From the construction point of view two types of CPCs have been used: the chambers stretched between the bases of common box, and self-supporting chambers in which a tension of the anode wires is applied to a thin-wall mylar supporting cylinder [7].

The chambers are from 360 to 600 mm long and from 128 to 1040 mm in diameter. The anode and cathode wires run along the elements of the cylinders inserted in one another. The wires are fixed on two ring flanges, each consisting of separate rings cast from a compound based on epoxy resin. The rings are reinforced with fiber glass laminate. During construction of the chamber, the rings are installed on the technological supporting cylinder. The stretched anode and cathode wires are fixed to the rings. The cathodes are made of beryllium bronze wires of 100 μm in diameter with spacing of 2 mm. The anodes are made of gold coated tungsten of 20 μm diameter with 1.96-2.36 mm spacing. The chamber construction is shown in figs. 3, 4. When all wires are fixed on rings the chamber is transferred to the detector's box, fastened to the upper and lower bases of the box and the technological supporting cylinder is removed. The wire tension is

transferred from the inner support (pressure) on the outer support (tension). The chamber is consisting only of wires and mylar shells keeping working gas in the chamber. This technology has been used for chambers of the first type (the one-coordinate chambers). The azimuthal coordinate of an event is determined according to the sequential signal wire number.

The two-coordinate chambers are made of self-supporting structure (figs. 3, 4). Their flanges are glued to a thin wall supporting cylinders made of several mylar layers. The cylinder ensures the necessary stability of the chamber when the anode wires are being tightened. The cathodes are made of mylar cylinders covered on the inner side with a graphite-based poorly conducting compound. The resistance of the cathode surfaces depends on the thickness of the sprayed conducting layer and is about 100 $k\Omega/_{\square}$. This should allow to regenerate the cathode potential at a large load capacity of the chamber ($\sim 10^4$ particles·wire·s^{-1}) and to ensure a reasonable signal height induced on strips (the threshold of preamplifiers is 0.5 mV). The helical conducting strips of aluminium (7 and 9 mm wide and 6 μm thick) are made on the outside of cylinders. The strips are isolated from the cathode conducting surface and earthed through a 10 kΩ resistor. The strips on the inner and outer cathodes are curled in opposite directions. Processing of signals induced on the strips allows one to determine two coordinates of the event and to get the information from the triggered anode wires.

The self-supporting CPC has a simpler design and convenience in assembly. Owing to these advantages, the one-coordinate chambers No. 2 and 3 are also made as self-supporting ones on the common supporting cylinder.

2.1.2. The wiring accuracy

The construction parts of chambers should have minimal dimensions, but they should be strong enough to keep wires in their positions as the tension on rings is 2-3 kg cm^{-1} and the total tension of all wires in the detector is ~ 4 tons. A possible deformation of construction parts should not influence considerably the performance of the wires. However, there are other effects such as an electrostatic effect, a gravitational effect, a temperature effect and an inaccurate positioning of wires that could influence their performance.

To keep the electrostatic effect at minimum the wire tension should be

$$T > \frac{H^2 V^2}{\pi^2 (R_2 - R_1)^2},$$

where H is the wire length, V is the high voltage, R_1 and R_2 is the corresponding cathode radius.

The wire distortion at the centre due to the gravitational effect can be expressed as

$$h = \frac{g l^2}{8T},$$

where g is the mass of the unit wire length and l is the wire length. The distortion of anode wires of 20 μm diameter is negligible. However, for cathode wires of 100 μm diameter the gravitational distortion is comparable with the electrostatic one. Taking into consideration these facts the tension of anode wires has been

chosen 35, 40 and 45 g, and cathode wires 120, 130 and 150 g, depending on the wire length. The wire distortion at the centre is controlled during the chamber construction by inserting a tensor at the centre. The accuracy is ±1 and ±2 % at the tension of 150 and 50 g, respectively.

The wire tension in chambers inserted in the box is controlled electronically using the frequency of wire self oscillations

$$f = \frac{\pi}{l}\sqrt{\frac{T}{s\rho}},$$

where s is the wire cross section and ρ is the wire material density.

The distance between wires and wire layers, parallelism of wires with the chamber's axis and the cylindrical shape of wire layers have been optically measured with the precision of ±0.05 mm.

2.1.3. The gas filling

The gas filling of chambers should enable to work at a relatively low working voltage, at a high counting efficiency, at a low noise and at a high gas amplification coefficient (up to 10^6). These requirements have been well fulfilled with the gas mixture argon (82.6 %) + isobutane (17 %) + freon (0.4 %). The chambers have been operated in the gas flow regime under a pressure of ~0.1 MPa. The admixture of isobutane in the gas filling may cause problems if the gas is released to the air, because 1.8-8.4 % of isobutane in the air forms an explosive mixture. Therefore a monitoring system has been developed to control an admixture of isobutane in the box. The monitor is based on a small volume ionization chamber that uses the box air as the working gas [8]. A small admixture of isobutane (>0.8 %) in the air considerably increases the current in the chamber that triggers the alarming system.

2.1.4. The working characteristics

Working voltages of chambers are within 1.8-4.5 kV, depending on the anode-cathode distance, the anode spacing and the gas filling. Typical currents in the chamber are between 5-150 μA, depending on the chamber construction and the load statistics. A negative high voltage is fed through the 0.5 MΩ resistance to cathodes.

The working characteristics of proportional chambers have been investigated on a computer-controlled stand. β-rays and cosmic rays monitored by two scintillation detectors have been used to check the performance of chambers. A chamber efficiency, a wire response, a beam profile and registration of clusters have been checked for each chamber. Almost 100 % counting efficiency has been obtained for all chambers. The chambers have a long plateau and stable noise characteristics. Fig. 5 shows a typical working characteristics of chambers. The wire beam profile and the cluster distribution is shown in fig. 6.

The technique developed for CPC allows to obtain a maximum transparency and solid angle of the detector. The basic parameters of CPC are given in table 2. Brackets denote two-chamber blocks made as a whole. The total number of signal wires is ~15000. The anode wires are grouped in 32 channels for unification of the electronics. Very good results obtained with CPC confirmed the successful design and construction features of chambers. Very thorough chamber construction and

pre-investigation before chamber installation in the box enabled to reach very reliable chamber operation in long term experiments. In five years of spectrometer operation only 3 wires has been broken.

2.2. The cylindrical scintillation hodoscopes

The scintillation hodoscopes consist of 36 scintillation counters grouped into three rows arranged between CPC, fig. 2. The first row of 4 scintillation counters is located on the 120 diameter (inside the first chamber), the second row of 8 counters is on the 245 diameter (between the third and the fourth chamber), and the third row of 24 counters is on the 670 mm diameter (between the 12th and 13th chamber). The length of scintillation counters is 360, 500 and 600 mm, respectively. The scintillation counters are made of 5 mm thick sheets of polystyrene with 2 % of terphenyl and 0.02 % of POPOP additives [9]. Light pulses proceed to photomultipliers XP 2020 (magnetically shielded) through light guides 1300 mm long. The time resolution is 1 ns for particles crossing the centre of a scintillation counter.

2.3. The gamma-detector

When studying decays with emission of γ-quanta a converter, diameter of 660 mm is inserted between the 12th and 13th chambers. Actually, the detector then consists of two parts - the detector of charged particles, and the detector of γ-quanta. With a magnetic field of 1.7 T tracks of charged particles from decays of stopped pions and muons are completely turned up in front of the converter at the radius 320 mm. The γ-detector is situated between the converter and the outer wall of the box (from the radius 345 to 530 mm) and consists of the converter and the chambers No. 13 to 18. The converter is made of lead or iron and the thickness depends on required energy resolution and registration efficiency of γ-quanta. Electron-positron pairs from gamma conversion are completely turned up in the γ-detector. This allows an accurate measurement of the radius of tracks.

The converter is not installed during studies of pion and muon interactions with nuclei. In this case charged particles are registered in all 18 proportional chambers. The γ-detector is also not used during a search for $\mu\rightarrow eee$, $\pi\rightarrow e\nu$ and $\pi\rightarrow 3e\nu$ decays. In this case an absorber is placed instead of the chambers No. 13-17, and the chamber No. 18 can be used as an anticoincidence shield. Fig. 7 shows the spectrometer arrangement for registration of charged particles only (a), as well as for both the charged particles and γ-quanta registration.

2.4. The magnet

The detection part of the spectrometer is placed in the magnet with the field up to 1.8 T (at a current of 2000 A and a voltage of 450 V). The cylindrical working region is 1080 in diameter and 1000 mm long. In the inserted poles of the magnet there are holes for cables from proportional chambers, and provision for placing light guides, and ejecting beams along the solenoid axis. It is also possible to inject a beam between coils at right angles to the solenoid axis. Field inhomogenity in the detection volume is less than 1 %.

2.5 The electronics and data acquisition system

The signals from proportional chambers are fed into the electronics through special band cables 2.4 m long. Each cable contains 32 signal wires made from gold coated tungsten of 30 μm diameter.

The electronics for the proportional chambers is based on large-scale hybrid integrated circuits (K405XP1). Each circuit includes all necessary electronics for two wires of proportional chambers. The integrated circuits are mounted on the PSI-32M boards with the dimensions of 200x270 mm, 16 IC's on each board (32 channels). The PSI-32M boards are arranged in crates, 33 boards (1056 channels) in one crate. On the magnet yoke 15 such crates are placed (15840 channels) [10].

The pulses from the cathode strips after preamplification are transmitted to the amplitude analysis modules KA-008 [11].

The trigger system uses information from the proportional chambers and scintillation hodoscopes. Since the detection system has many elements and multiparticle events are registered, the majority logic is used. To select the required combinations, standard units of fast logic and circuits of rapidly programmed memory are used [12]. Control elements and standard computer-controlled units of fast logic allow a rapid change of trigger logic, selection of delays, control over operation of photomultipliers, proportional chambers and other systems. When the fast logic unit produces a starting signal, information from the proportional chambers is recorded in the memory. At the same time information from some proportional chambers reaches a special-purpose processor RASTR [13] with ring shift registers. The processor finds out if there are tracks corresponding to the expected events. The processor RASTR works as the second stage trigger. It permits the spectrometric information read out to the computer.

The information from the spectrometer is collected firstly in one of the two fast switching (~ 1 μs) buffer memories KL-006, [14], and then in a SM-4 computer. The events are filtered using a special fast algorithm [15], requiring that an event has at least one negative and two positive tracks (in the case of the $\mu \rightarrow 3e$ experiment) passing through the target with the curvature within certain limits. After the filtration the events are fed into an EC-1040 computer, connected to the SM-4 via DMA channel, and recorded on a magnetic tape [16].

A data processing has been done in several steps with EC-1040, EC-1060, VAX-8350 and personal computers [17,18].

3. The first experiments with the ARES spectrometer

3.1. Search for $\mu \rightarrow 3e$ decay

The first experiment performed with the ARES spectrometer was a search for $\mu \rightarrow 3e$ decay [17]. The scheme of the experiment at the JINR phasotron is shown in fig. 8. The detector arrangement in this experiment is shown in fig. 9. The efficiencies of the proportional chambers No. 1-6, 9-12, as measured in this experiment, are listed in table 3. The chambers No. 7 and 8 were not used in this experiment. The total efficiency of three point events registered in three basic chambers (No. 1,4,9) is

$$\eta_{\Sigma} = \prod_{i=1,4,9} \eta_i^3 = 0.74.$$

The standard deviation of the track's coordination in the plane perpendicular to the chamber axis is $\sigma=\pm 0.7$ mm, and along the axis (the z-coordinate) is $\sigma_z=\pm 2$ mm. A detector trigger requires a coincidence of hits in 2 or more scintillation counters of 2nd row, 3 or more scintillation counters in 3rd row and 3 or more wires in the cathode strip chambers 1, 4 and 9. Besides, the fast memory was programmed to register only the events with the tracks in both hemispheres surrounding the target.

The computer reconstruction of three tracks events in R-φ and R-Z planes is shown in fig. 10. The relative decay probability as obtained in the experiment is given as

$$R_{\mu\to 3e}=\Gamma(\mu^+\to e^+e^-e^+)/\Gamma(\mu^+\to e^+\nu_e\bar{\nu}_\mu) \le 3.6\cdot 10^{-11}.$$

The full experiment description and discussion of results has been published elsewhere [17,18].

3.2. Investigation of $\pi^+\to e^+\nu_e e^+e^-$ decay

The same experimental arrangement as in the $\mu\to 3e$ experiment was used for investigation of the $\pi^+\to e^+\nu_e e^-e^+$ decay. The partial decay probability has been determined as

$$R=\Gamma(\pi\to e\nu ee)/\Gamma(\pi\to\mu\nu) \approx (4.6\pm 1.6\pm 0.7)\cdot 10^{-10}.$$

The description of the experiment and discussion of results has been given in [19].

4. Conclusion

The experimental facility ARES has been in reliable full operation since 1988 using the JINR phasotron meson beam and it has produced first physics results. The novel cylindrical proportional chambers, a heart of the spectrometer, after careful design, construction and testing have shown successful long-term operation in the ARES facility. At present the facility is used for investigation of rare pion interactions with nuclei.

Acknowledgment

The authors are grateful to B. Kuehn, V. I. Komarov, G. A. Kosarev, S. V. Medved, G. V. Mitzelmakher, J. Polach, A. N. Sinaev and V. G. Zinov for for helpful discussions and assistance.

References

[1] Proc. the 14th Europhysics Conference on Nuclear Physics, Part A: Rare Nuclear Decays and Fundamental Processes, J. Phys. G 17(1991)S1-S543; Part B: Rare Nuclear Processes, ed. P. Povinec (World Scientific, Singapore, 1992).
[2] U. Bellgardt et al., Nucl. Phys. B299(1988)1.
[3] R.D. Bolton et al., Phys. Rev. D38(1988)2077.
[4] A.Badertscher et al., J. Phys. G 17(1991)S47.
[5] S.M. Korenchenko et al., JINR preprint P13-9542, Dubna (1976).
[6] N.P. Kravchuk et al., JINR preprint P13-11862, Dubna (1978).
[7] A.S. Korenchenko et al., JINR preprint P13-83479, Dubna (1983).
[8] J. Vanko et al., JINR preprint P13-87-764, Dubna (1987).
[9] V.A. Baranov et al., Prib. Tekh. Eksp. 6(1987)40.
[10] S.M. Korenchenko et al., JINR preprint P13-11561, Dubna (1978).
[11] V.A. Antyukhov et al., JINR preprint P10-12912, Dubna (1979).
[12] V.A. Baranov et al., Proc. Int. Conf. Nuclear Electronics (JINR, Dubna (1985)p. 28.
[13] V.A. Baranov et al., JINR preprint P13-82-768, Dubna (1982).
[14] V.A. Antyukhov et al., JINR preprint P10-80-650, Dubna (1980).
[15] P.G. Evtukhovich et al., JINR preprint P10-85-383, Dubna (1985).
[16] V.A. Baranov et al., JINR preprint P13-81-162, Dubna (1981).
[17] V.A. Baranov et al., Yad. fizika 53(1991)1302.
[18] V.A. Baranov et al. J. Phys. G 17(1991)S57.
[19] V.A. Baranov et al.,Yad. Fizika 55(1992)2940.

Table 1
Parameters of the ARES spectrometer

Detector diameter [mm]	1060
Detector length [mm]	600
Number of cylindrical proportional chambers	18
Number of information channels	~15000
Number of scintillation detectors	36
Magnetic field [T]	<1.8
Solid angle [sr]	0.7x4π
Space resolution [mm]	<2
Time resolution [ns]	1
Accuracy of γ-quantum energy determination [%]	1-5
Accuracy of $e^{\pm}$ energy determination (70 MeV) [%]	2
Loading statistics [events/s]	<100

Table 2
The main parameters of CMPC used in the ARES spectrometer. The thickness of the chambers is given without the gas.

Chamber	Anodic cylinder diameter (mm)	No. of anode wires	Anode wire spacing (mm)	Anode cathode gap (mm)	Chamber (wire) length (mm)	Cathode type [a]	No. of strips in layer			Strip/wire angle (deg) in layer			Chamber thickness	
							1	2	3	1	2	3	10^{-2} g/cm^2	10^{-4} rad. length
1	128	192	2.09	2.5	360	I	32	32	16	54.55	−46.51	90	7.1	18.5
2	164	256	2.01	6	400									
3	212	320	2.08	6	400	II	–	–	–	–	–	–	13.8	42.3
4	274	384	2.24	4	500	I	48	48		58.83	−60.87		11.2	28.5
5	319.6	480	2.09	6	500									
6	343.6	512	2.11	6	500	II	–	–	–	–	–	–	3.8	15.6
7	405.5	640	1.99	6	500									
8	429.5	672	2.01	6	500	II	–	–	–	–	–	–	3.8	15.6
9	478.8	768	1.96	4	600	I	96	96		58.78	−59.97		13.6	34.7
10	539.3	768	2.21	6	600									
11	563.3	768	2.30	6	600	II	–	–	–	–	–	–	3.8	15.6
12	629.2	960	2.06	6	600	II	–	–	–	–	–	–	3.5	12.5
13	702.2	1152	1.92	6	600	I	128	128		57.89	−59.12		18.2	46.3
14	758	1152	2.07	6	600									
15	782	1152	2.13	6	600	II	–	–	–	–	–	–	3.8	15.6
16	841.9	1152	2.30	6	600									
17	865.9	1152	2.36	6	600	II	–	–	–	–	–	–	3.8	15.6
18	1038.7	1536	2.12	6	600	II	–	–	–	–	–	–	3.5	12.5
Σ	–	14016	–	–	–	–	–	–	–	–	–	–	89.9	273.3

[a] I: continuous; II: wire.

Table 3
Efficiency of cylindrical proportional chambers

CPC	1	2	3	4	5	6	9	10	11	12
η	0.946	0.983	0.962	0.972	0.969	0.976	0.984	0.920	0.966	0.943

Figure captions

Fig. 1. Scheme of the ARES spectrometer. General view. 1 - target, 2 - cylindrical proportional chambers, 3 - cylindrical scintillation hodoscopes, 4 - light guides, 5 - photomultipliers, 6 - electronics for CPC, 7 - magnet's winding, 8 - magnet's yoke, 9 - magnet's poles.

Fig. 2. Cross section of the detection part. 1 - target, 2 - signal wire layers of CPC (points marking two-coordinate CPC), 3 - plastic scintillators, 4 - γ-converter, 5 - positron track, 6 - electron-positron pair track.

Fig. 3. Construction of (a) one-coordinate and (b) two-coordinate chambers. 1 - chamber flanges, 2 - supporting cylinder, 3 - anodes, 4 - cathodes, 5 - supporting box.

Fig, 4. Cross section of (a) one-coordinate chamber. 1 - chamber flanges, 2 - removable supporting cylinder, 3 - cathode wires, 4 - anode wires, 5 - mylar shells (100 μm), 6 - protective rings, 7 - soldering of cathode wires, 8 - plates for soldering of anode wires.
(b) two-coordinate chambers. 1 - chamber flanges, 2 - supporting cylinder, 3 - fixing point.

Fig. 5. Typical working characteristics of CPC. 1 - efficiency, 2 - noise.

Fig. 6. A chamber test on the automatized stand. (a) beam profile, (b) distribution of clusters.

Fig. 7. Cross section of the spectrometer for charged particles registration (a) and for both charged particles and γ-quanta registration (b).

Fig. 8. ARES arrangement at the JINR phasotron.

Fig. 9. Spectrometer arrangement for the $\mu \rightarrow 3e$ experiment. 1 - scintillation counter, 2 - moderator, 3 - target, 4,5,6 - scintillation hodoscopes, 7 - self-supporting chamber, 8 - double-stretching chamber, 9 - signal cables, 10 - regulation point of the stretching chamber, 11 - supporting cylinder of the self-supporting chamber, 12 - strips, 13 - anode wires, 14 - cathode wires, 15 - protective covers, 16 - absorber, 17 - box of the detection part.

Fig. 10. Reconstruction of typical three-tracks events.

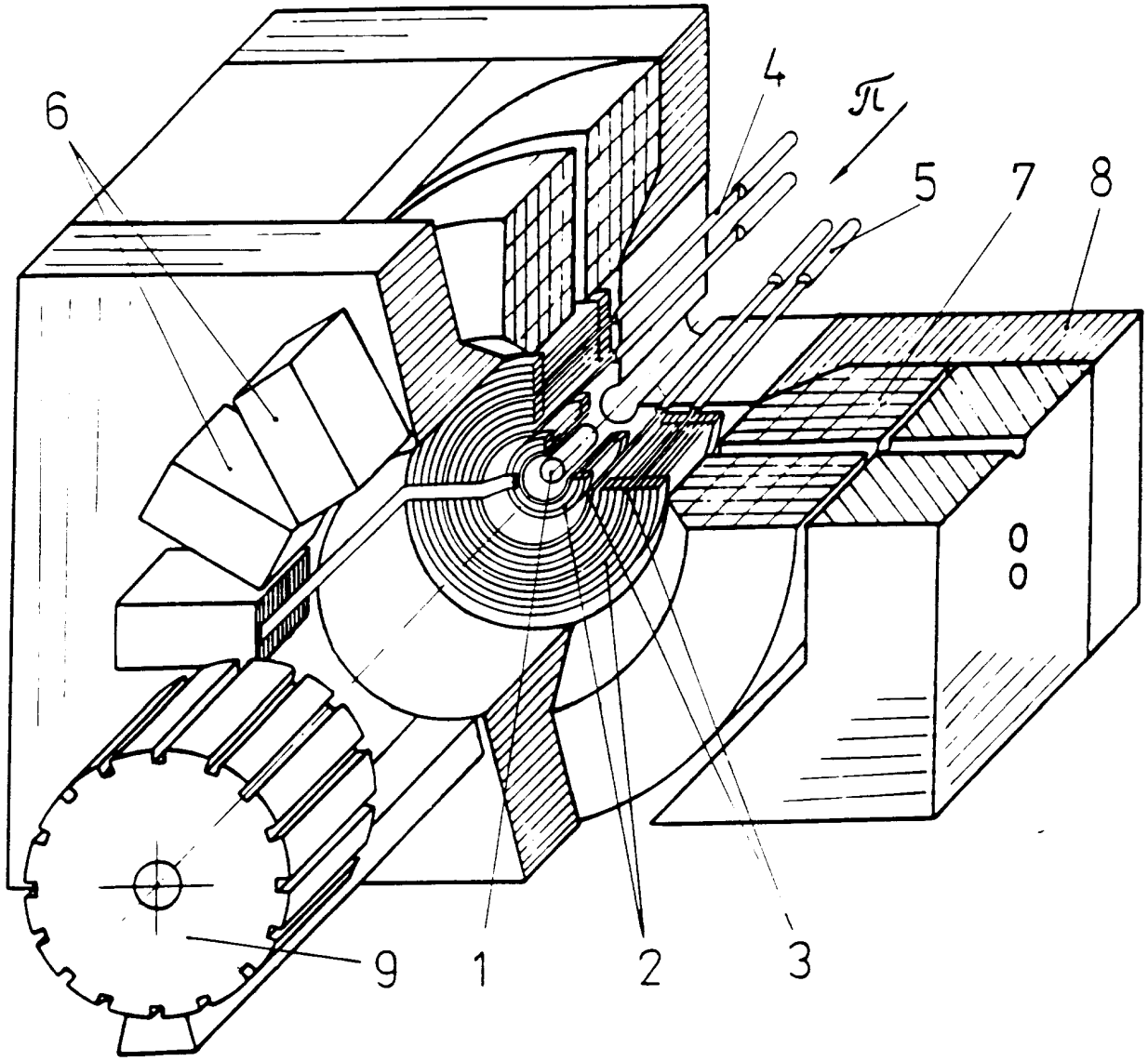

Fig. 1

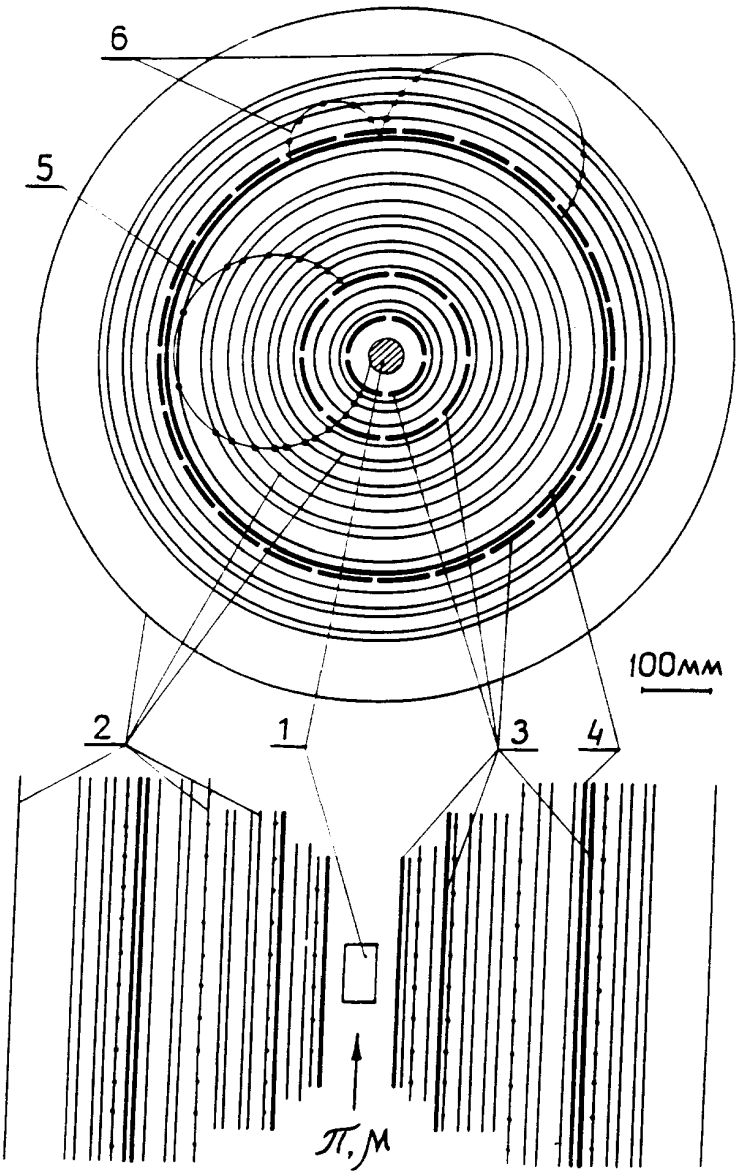

Fig. 2

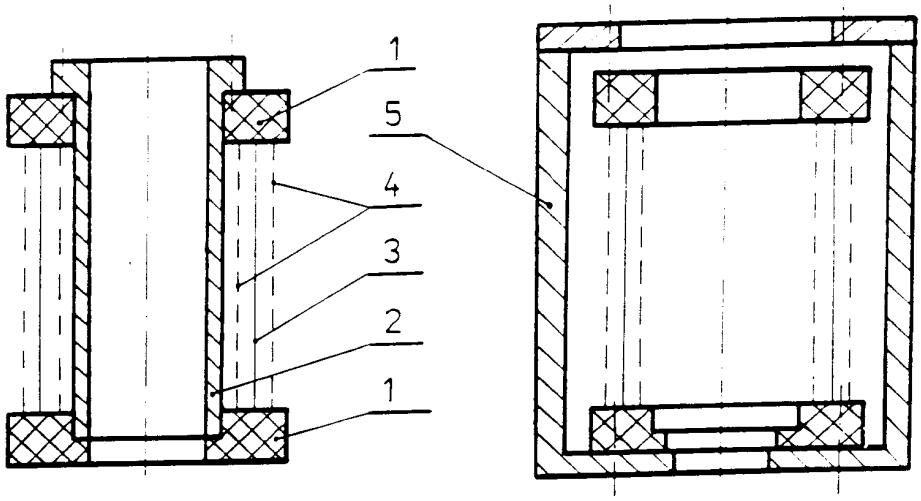

Fig. 3

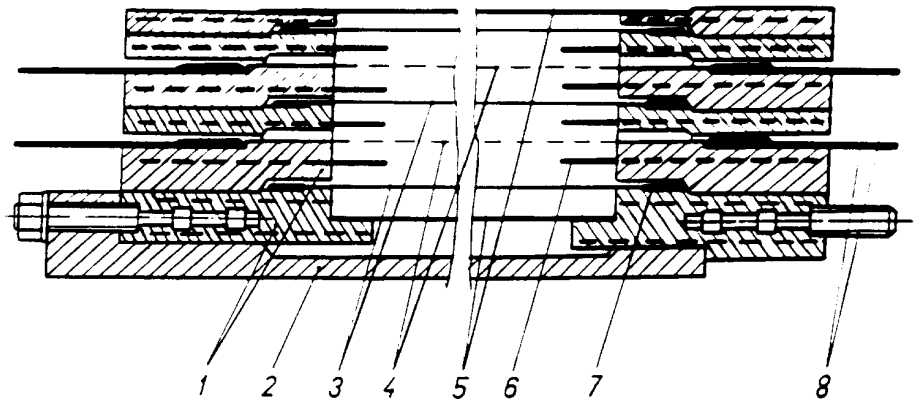

(a)

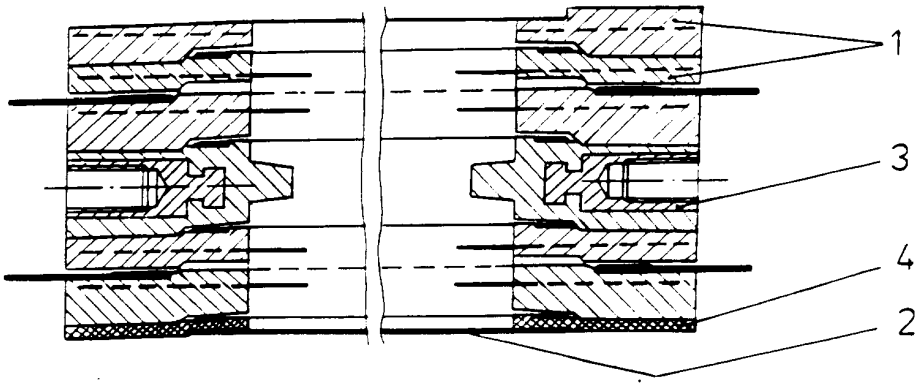

(b)

Fig. 4

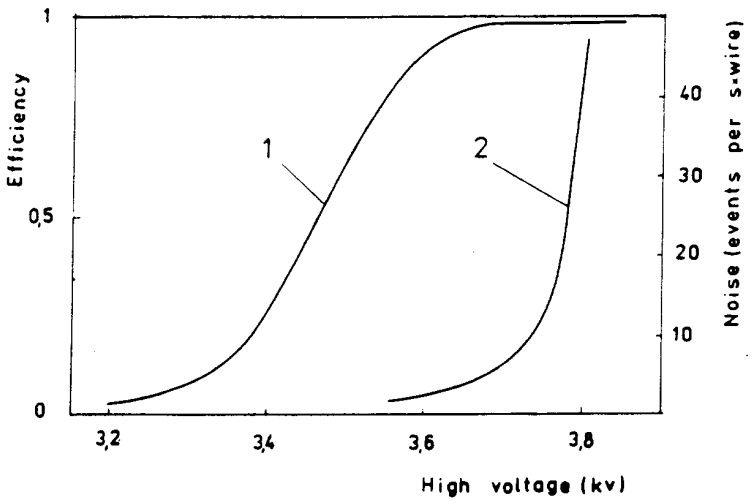
1
0,5
0
Efficiency
1
2
40
30
20
10
Noise (events per s-wire)
3,2
3,4
3,6
3,8
High voltage (kv)

Fig. 5

(a) beam profile

```
20   1     0
20   2     1   *
20   3     1   *
20   4     0
20   5     1   *
20   6     1   *
20   7     3   *
20   8    13   *
20   9    19   **
20  10    83   ***********
20  11   199   ****************************
20  12   328   ***********************************************************
20  13   202   ****************************
20  14    85   ***********
20  15    21   ***
20  16     9   *
20  17     2   *
20  18     1   *
20  19     3   *
20  20     1   *
20  21     1   *
20  22     1   *
20  23     0
20  24     1   *
20  25     0
20  26     0
20  27     1   *
20  28     0
20  29     0
20  30     1   *
20  31     0
20  32     0
```

(b) cluster events %

```
1          871   88.606    ********************
2          104   10.579    ***
3            4    0.407    *
4            3    0.305    *
5            1    0.102    *
```

Fig. 6

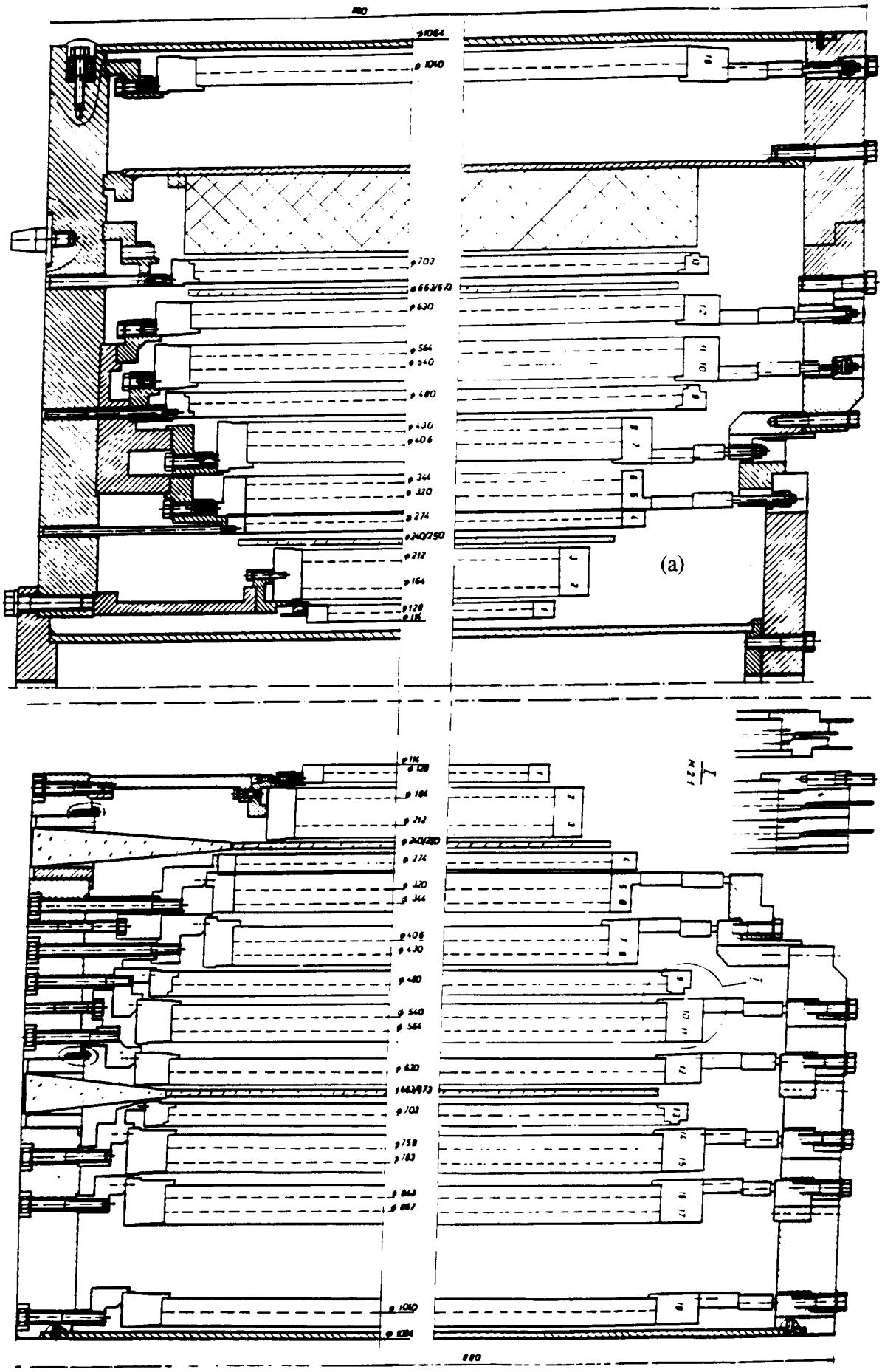

Fig. 7 (b)

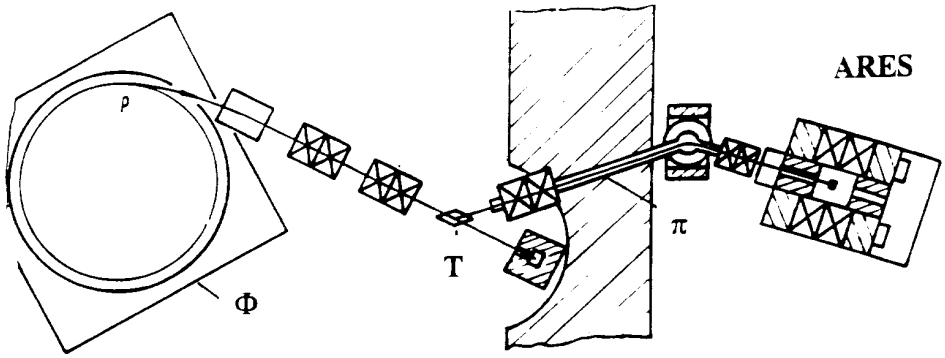

Fig. 8

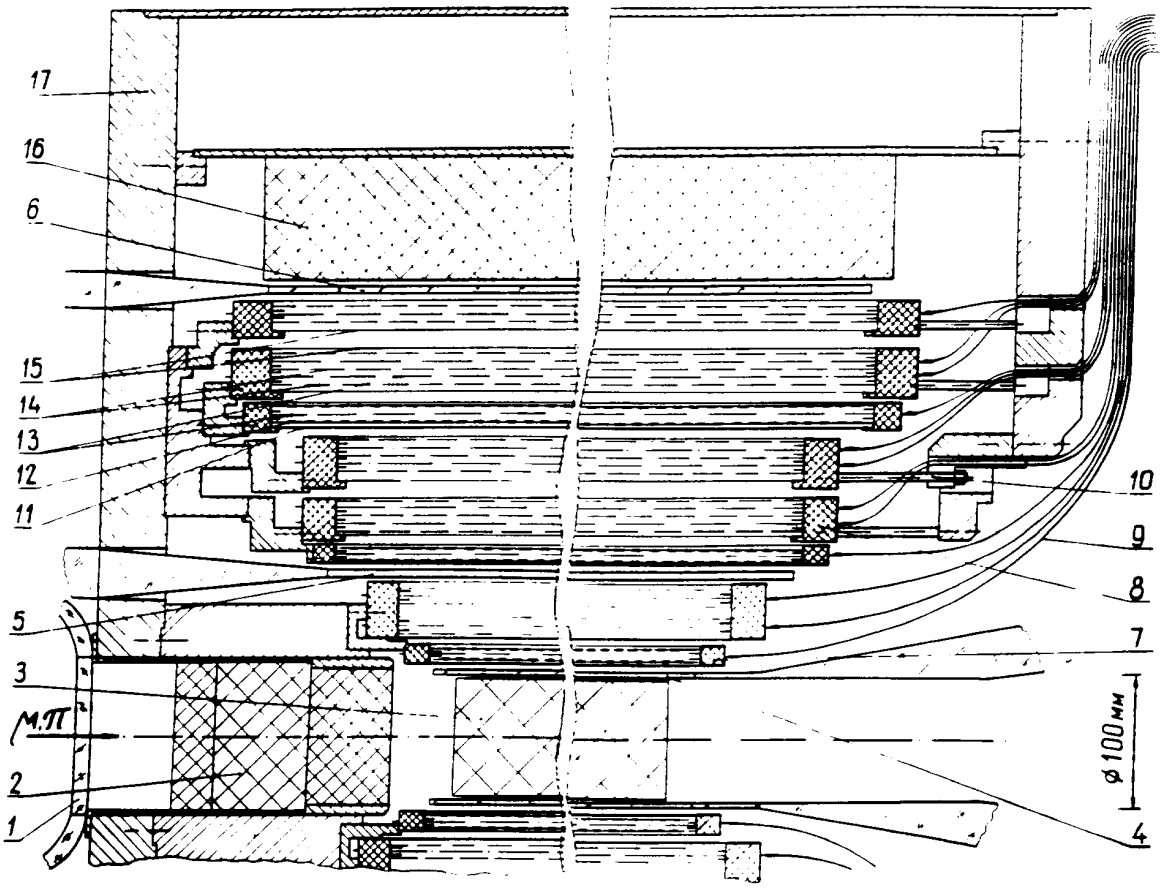

Fig. 9

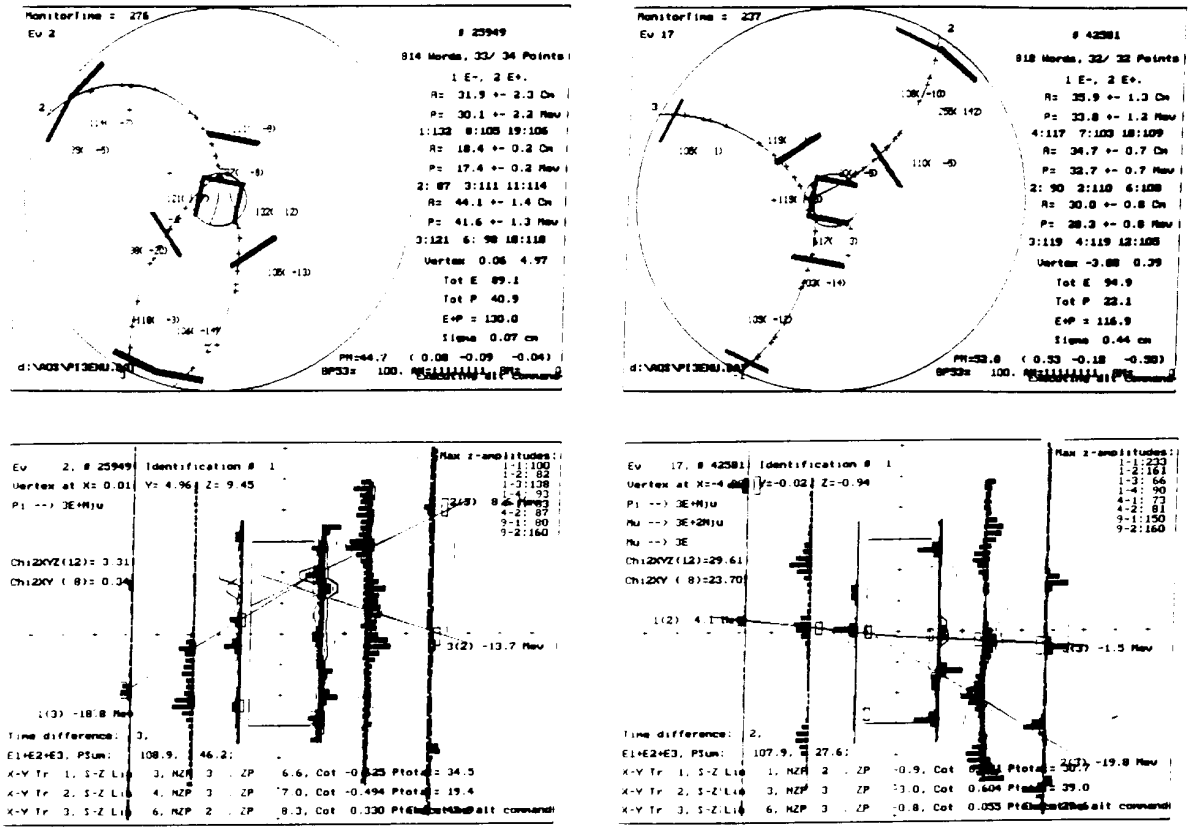

Fig. 10